

Supporting Information

Structure-Kinetic Relationship Study of Organozinc Reagents

Guanghai Zhang,^{a, b} Jing Li,^a Yi Deng,^{a, b} Jeffrey T. Miller,^b A. Jeremy Kropf,^b Emilio E. Bunel,^b
and Aiwèn Lei^{a, b, c, *}

^a College of Chemistry and Molecular Sciences, Wuhan University, Wuhan, Hubei 430072, P. R. China

aiwenlei@whu.edu.cn

http://aiwenlei.whu.edu.cn/mail_website/

^b Chemical Sciences and Engineering Division, Argonne National Laboratory, 9700 S. Cass Ave., Argonne,
IL 60439, US

^c State Key Laboratory of Organometallic Chemistry, Shanghai Institute of Organic Chemistry, Chinese
Academy of Sciences, 354 Fenglin Lu, Shanghai 200032, P. R. China

Contents

| | |
|--|-----|
| General Information | S3 |
| XANES and EXAFS Data Collection and Analysis | S3 |
| Table S1 Edge Energy | S5 |
| Table S2 Structural Parameters of XAS Standard Samples | S6 |
| Figure S1 Fitting results of the k^2 -weighted R-space EXAFS spectrum of ZnI_2 /THF solution. | S6 |
| IR Data Collection | S7 |
| Experimental Details | S7 |
| Confirmation of transmetallation as the rate-limiting step | S8 |
| Figure S2 kinetics of various phenylzinc reagents in oxidative homocoupling reaction | S9 |
| Table S3 Initial rates of oxidative homocoupling reactions using various phenylzinc reagents | S10 |
| Figure S3 Kinetics of Pd-catalyzed Negishi-type oxidative homo-coupling reaction of phenylzinc reagent I | S10 |
| Figure S4 Kinetics of Pd-catalyzed Negishi-type oxidative homo-coupling reaction of phenylzinc reagent II | S11 |
| Table S4 Initial rates of oxidative homocoupling reactions using various phenylzinc reagent concentrations | S11 |
| Further discussion on the relationship between the structure and reactivity | S11 |
| Figure S5 Possible transmetallation pathways. | S13 |
| References | S13 |

General Information

All manipulations were carried out either in a glovebox or using standard Schlenk techniques. All glassware was oven dried at 120 °C for more than 1 hour prior to use. THF was dried and distilled from sodium/benzophenone ketyl in nitrogen atmosphere. Anhydrous ZnCl₂, ZnBr₂ and ZnI₂ were from commercial source (Sigma-Aldrich) and used as received without further purification. Commercially available phenyllithium reagent and Pd(OAc)₂ were used as received. GC analysis was done on a Varian GC 3900 gas chromatography instrument with a FID detector. GC-MS spectra were recorded on a Varian GC-MS 3900-2100T.

XANES and EXAFS Data Collection and Analysis

X-ray absorption measurements were acquired on the insertion device beam line of the Materials Research Collaborative Access Team (MRCAT) at the Advanced Photon Source, Argonne National Laboratory. The data were collected in transmission quick scan mode. Insertion device experiments utilized a cryogenically cooled double-crystal Si (111) monochromator in conjunction with an uncoated glass mirror to minimize the presence of harmonics. The monochromator was scanned continuously during the measurements with data points integrated over 0.5 eV for 0.03 s per data point. The ionization chambers were optimized for the maximum current with linear response ($\sim 10^{10}$ photons detected/sec) with 10% absorption (N₂) in the incident ion chamber and 70% absorption (50% N₂ and 50% Ar) in the transmission detector. A Zn foil spectrum (edge energy 9659 eV) was acquired simultaneously with each measurement for energy calibration and multiple scans were taken to ensure spectrum reproducibility.

All of the solution samples were prepared in a glove box and placed in a sample holder made of PEEK (polyether ether ketone) equipped with a screw top and O-ring fitting to prevent exposure to air and water.¹ The path length of the cell is 3.5 mm and the Zn concentration was adjusted to be about 0.1 M.

ZnI₂/THF solution: In a glovebox, ZnI₂ (319 mg, 1.0 mmol) was dissolved in 10 mL of dry THF. Then 3 mL of the solution was then transferred into the solution cell and sealed. XAS spectrum was then measured at room temperature.

ZnBr₂/THF solution: In a glovebox, ZnBr₂ (225 mg, 1.0 mmol) was dissolved in 10 mL of dry THF. Then 3 mL of the solution was then transferred into the solution cell and sealed. XAS spectrum was then measured at room temperature.

ZnCl₂/THF solution: In a glovebox, ZnCl₂ (136 mg, 1.0 mmol) was dissolved in 10 mL of dry THF. Then 3 mL of the solution was then transferred into the solution cell and sealed. XAS spectrum was then measured at room temperature.

[PhZnI₂(THF)]Li: In a glovebox, a small vial (20 mL) was charged with ZnI₂ (319 mg, 1.0 mmol) and 9.5 mL of dry THF. After all the solid was dissolved, 0.53 mL of PhLi (1.9M, 1.0 mmol) was added. Then the solution was stirred at room temperature for 10 minutes in the glovebox. 3 mL of the obtained solution was transferred into the solution cell and sealed. XAS spectrum was measured at room temperature.

[PhZnBr₂(THF)]Li: In a glovebox, a small vial (20 mL) was charged with ZnBr₂ (225 mg, 1.0 mmol) and 9.5 mL of dry THF. After all the solid was dissolved, 0.53 mL of PhLi (1.9M, 1.0 mmol) was added. Then the solution was stirred at room temperature for 10 minutes in the glovebox. 3 mL of the obtained solution was transferred into the solution cell and sealed. XAS spectrum was measured at room temperature.

[PhZnCl₂(THF)]Li: In a glovebox, a small vial (20 mL) was charged with ZnCl₂ (136 mg, 1.0 mmol) and 9.5 mL of dry THF. After all the solid was dissolved, 0.53 mL of PhLi (1.9M, 1.0 mmol) was added. Then the solution was stirred at room temperature for 10 minutes in the glovebox. 3 mL of the obtained solution was transferred into the solution cell and sealed. XAS spectrum was measured at room temperature.

Each solid sample was mixed with boron nitride to a weight ratio of about 2% (Zn) in the glove box. The mixture was grinded well with mortar and pestle, and then 25 mg of the mixture was pressed into a cylindrical sample holder consisting of six wells with a radius of 2.0 mm, forming a self-supporting wafer. The sample holder was placed in a quartz tube (1-in. OD, 10-in.

length) sealed with Kapton windows by two Ultra-Torr fittings and then used for transmission mode measurement.

The edge energy of the X-Ray absorption near edge structure (XANES) spectrum was determined from the inflection point in the edge, i.e., the maximum in the first derivative of the XANES spectrum. Experimental phase shift and back scattering amplitude were used to fit the EXAFS data. Zn-O, Zn-Cl, Zn-Br and Zn-I phase shifts and back scattering amplitudes were obtained from reference compounds: ZnO (4 Zn-O at 1.98 Å), ZnCl₂ (4 Zn-Cl at 2.34 Å), ZnBr₂ (4 Zn-Br at 2.42 Å) and ZnI₂ (4 Zn-I at 2.62 Å), respectively.²⁻⁴ Zn-O phase shift and back scattering amplitude were used to fit both Zn-O and Zn-C shells. Since EXAFS can't tell the difference between oxygen and carbon. In the fitting process, we assume that Zn-C bond is shorter than Zn-O bond, since C is the phenyl anion, while O represents the neutral THF.

Background removal and normalization procedures were carried out using the Athena software package using standard methods.⁵ Standard procedures based on WinXAS 3.2 software were used to extract the extended X-ray absorption fine structure (EXAFS) data.⁶ Fourier filtering technique was used to remove the features below 1 Å in the R-space spectra. The coordination parameters were obtained by a least square fit in R-space of the nearest neighbor, k²-weighted Fourier transform data. The data fit equally well with both k¹ and k³ weightings.

Table S1 Edge Energy

| Sample | Edge Energy (eV) | Sample | Edge Energy (eV) | Sample | Edge Energy (eV) |
|---------------------------------|------------------|---------------------------------|------------------|--------------------------------|------------------|
| ZnCl ₂ | 9662.6 | ZnBr ₂ | 9662.3 | ZnI ₂ | 9661.9 |
| ZnCl ₂ /THF Solution | 9662.4 | ZnBr ₂ /THF Solution | 9662.3 | ZnI ₂ /THF Solution | 9662.1 |
| [PhZnCl ₂ (THF)]Li | 9660.5 | [PhZnBr ₂ (THF)]Li | 9660.6 | [PhZnI ₂ (THF)]Li | 9660.4 |

Table S2 Structural Parameters of XAS Standard Samples

| Sample | Abs.-Bs. Pair | N | R (Å) |
|---------------------------|---------------|---|-------|
| ZnO (solid) | Zn-O | 4 | 1.98 |
| ZnCl ₂ (Solid) | Zn-Cl | 4 | 2.34 |
| ZnBr ₂ (solid) | Zn-Br | 4 | 2.42 |
| ZnI ₂ (solid) | Zn-I | 4 | 2.62 |

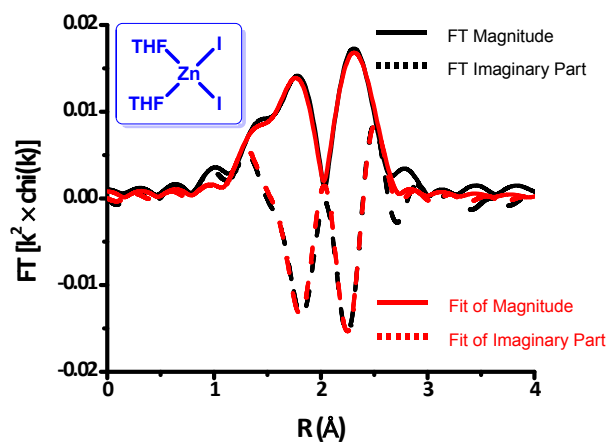


Figure S1 Fitting results of the k^2 -weighted R-space EXAFS spectrum of ZnI_2/THF solution.

Fourier transform (FT) range: $2.86 \text{ \AA}^{-1} - 11.88 \text{ \AA}^{-1}$; fitting range: $1.22 \text{ \AA} - 2.59 \text{ \AA}$.

IR Data Collection

Experimental Details

All reactions and manipulations were conducted in a nitrogen-filled self-prepared three-neck micro reactor. IR spectra were recorded on a Mettler Toledo ReactIR™ 15 spectrometer using a diamond comb. Yields of Ar-Ar were obtained from GC and naphthalene was added as internal standard. The concentration of organozinc reagent was determined by the titration by I₂/LiCl.

To a 50 mL round-bottom flask was added ZnX₂ (X=Cl, Br, I) (13 mmol,) and THF (as the solvent, 33.5 mL). The mixture was allowed to stir at 0 °C for 5 min. Phenyllithium (1.9 M, 12 mmol) was injected slowly to the flask *via* a syringe. The temperature was allowed to warm up to room temperature. After stirring for about 30 min, the arylzinc reagent concentration was determined based on the titration by I₂ / LiCl.

In an oven dried home-made three-neck reactor with a magnetic stirrer, naphthalene (30 mg) as the internal standard and 2-chloro-1,2-diphenylethanone (0.50 mmol, 115 mg) were added. The reactor was allowed to be vacuumed and purged with nitrogen for several times. The arylzinc reagent (0.25 M in THF, 4.0 mL) was added *via* a syringe. The mixture was allowed to stir at indicated temperature and recorded by React IR. At the same time, Pd(OAc)₂ (5.6×10⁻⁵ M in THF, 100 μL) was added in quickly by a micro syringe. The course of the reaction could be observed from either the characteristic IR absorption of 2-chloro-1,2-diphenylethanone or that of the product biphenyl. When 2-chloro-1,2-diphenylethanone was consumed completely, the reaction was quenched by diluted hydrochloric acid and the yield of product was determined by GC.

Confirmation of transmetallation as the rate-limiting step

In the Pd-catalyzed Negishi-type oxidative homo-coupling reaction, the dependence of the initial rates on the concentration of phenylzinc reagent I and phenylzinc reagent II were tested, respectively. Monitored by *in situ* IR, the reaction rates were measured at 0 °C. A linear relationship was obtained by plotting the initial rates vs. the concentration of phenylzinc reagent, which suggests that the reaction rate is first-order dependent on the concentration of phenylzinc reagent. It confirmed that the rate-limiting step was the transmetallation. Details are shown below.

Generally, the mechanism for transition-metal catalyzed cross-coupling reactions is described as an accepted catalytic cycle involving three elementary steps: 1) oxidative addition of R-X to a low valent transition metal catalyst M to afford a [R-M-X] intermediate; 2) transmetallation between [R-M-X] and an organometallic reagent R'M to form [R-M-R']; 3) reductive elimination of [R-M-R'] to produce R-R' and low valent metal catalyst. In our model reaction, We investigated the kinetics in Pd-catalyzed Negishi-type oxidative homocoupling of ArZnX with desyl-chloride as oxidant. Desyl-chloride as the oxidant gave very fast oxidative addition, and transmetallation was determined as the rate limiting step. The detailed mathematics is shown below.

The characteristic absorption peaks of desyl-Cl (1705 cm^{-1} , C=O) and biphenyl (743 cm^{-1}) were monitored in the *in situ* IR experiments, and the amount of desyl-Cl and biphenyl were quantitated by GC after the reaction was quenched. What we got from the *in situ* IR experiments was the relationship of absorbance vs reaction time, and then we converted the absorbance into the concentration of desyl-Cl.

At the beginning of reaction, the concentration of desyl-Cl is C_0 ; at the end of the reaction, the concentration is C_e , and C_t is used for the concentration during the reaction process.

According to the Lambert-Beer's law:

$$A_0 = k C_0 \quad \text{Eq.1}$$

$$A_e = k C_e \quad \text{Eq.2}$$

$$A_t = k C_t \quad \text{Eq.3}$$

We can get $C_t = (A_e - A_t) * C_0 / (A_e - A_0)$

The reaction rate $r = (C_0 - C_t) / t$

It is known that Pd(OAc)₂ decays easily in the presence of organometallic reducing agents, so the initial rates should be used in the kinetic investigations. As shown in Figure S2, at the beginning of the reaction (60 s for phenylzinc reagent I and 300 s for zinc reagent II and III), the consumption of desyl-chloride showed a straight line which suggests that in the time period, no obvious decay of the Pd catalyst occurred. The obtained initial rate should be able to represent the "real" rate. Table S3 summarizes the initial rates of all the three phenylzinc reagents.

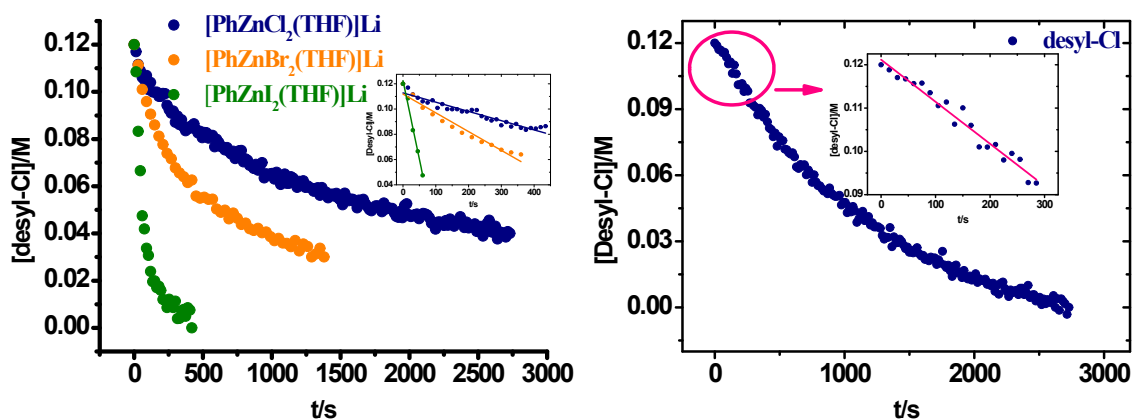


Figure S2 kinetics of various phenylzinc reagents in oxidative homocoupling reaction

Table S3 Initial rates of oxidative homocoupling reactions using various phenylzinc reagents

| organozinc reagent | initial rate/ 10^{-5} M/s |
|--------------------|-----------------------------|
| I | 125 |
| II | 14.9 |
| III | 7.32 |

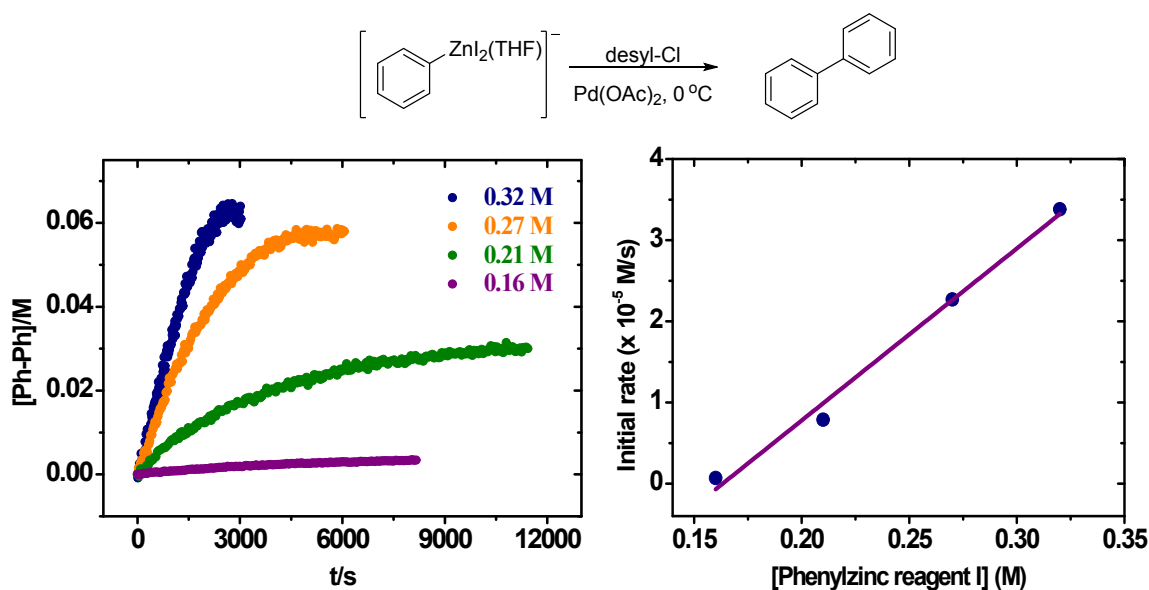


Figure S3 Kinetics of Pd-catalyzed Negishi-type oxidative homo-coupling reaction of phenylzinc reagent I.

Reaction condition: Phenylzinc zinc I (0.16 M-0.32 M, 6 mL), desyl-Cl (0.5 mmol), $\text{Pd}(\text{OAc})_2$ (3.7×10^{-5} M), 0°C .

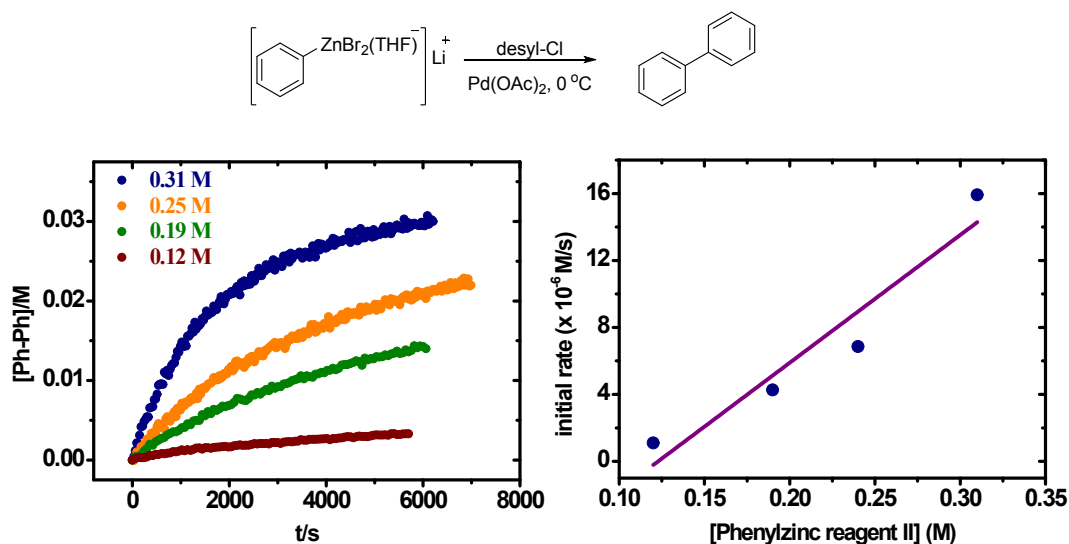


Figure S4 Kinetics of Pd-catalyzed Negishi-type oxidative homo-coupling reaction of phenylzinc reagent II.

Reaction conditions: Phenylzinc zinc II (0.12 M-0.31 M, 6 mL), desyl-Cl (0.5 mmol), Pd(OAc)₂ (3.7×10^{-5} M), 0 °C.

Table S4 Initial rates of oxidative homocoupling reactions using various phenylzinc reagent concentrations

| C(Phenylzinc reagent I)/M | initial rate / 10^{-5} M/s | C(Phenylzinc reagent II)/M | initial rate/ 10^{-6} M/s |
|---------------------------|------------------------------|----------------------------|-----------------------------|
| 0.16 | 6.92 | 0.12 | 1.10 |
| 0.21 | 7.87 | 0.19 | 4.27 |
| 0.27 | 2.26 | 0.24 | 6.86 |
| 0.32 | 3.38 | 0.31 | 15.9 |

Further discussion on the relationship between the structure and reactivity

All the three Zn species have very similar disordered tetrahedron coordination geometry, the difference of the Zn-C bond distance and the reactivity is probably caused by the electronic properties of the halide ligands.

- 1) The π bonding between Zn^{2+} and halide anion is not significant. Zn^{2+} cation has a d^{10} electronic configuration, where all the d orbitals of Zn are fully occupied. So the π bonding would lead to a net destabilization by the “filled-filled” interactions.
- 2) It is generally appreciated that the electronegativity of the halogens increases up the group as a consequence of the halide electronegativity and the availability of their s electrons. In the absence of π interactions between the halide anions and Zn^{2+} , iodide would be expected to donate the most electron density to the metal by σ interactions. Thus, for phenylzinc reagent I, the Zn-C bond will be most weakened by the resulting increase of electron density on Zn^{2+} . The highest transmetallation rate could also be expected.
- 3) Steric effect should also be taken into consideration when comparing the halide effect, since the relative size of the halide ligand sometimes plays a crucial role, especially when the halide is on metal complex with high coordination numbers⁷. For example, the rate of oxidative addition might be slowed down by replacing Cl^- by I^- due to the increase of the steric effect. However, in our case, transmetallation is the rate-limiting step, where no highly crowded intermediate is necessarily involved. So we believe the steric effect is not playing the key role in our case.
- 4) The *trans* effect is usually notable in square planar complexes. In our case, all the Zn^{2+} adopt disordered tetrahedron geometry, so we do not believe it is crucial, neither, although iodide gives stronger *trans* effect than bromide and chloride in most cases.

In summary, we believe the σ interaction between the Zn cation and the halide ligands plays the key role. The steric effect and *trans* effect may also affect the Zn-C bond distance and the reactivity of the phenylzinc reagent, but they are not dominating the reactivity.

As discussed, the *in situ* IR experiments demonstrated that transmetallation was the rate limiting step in the oxidative homocoupling reaction, so the breaking the Zn-C bond and forming the Pd-C bond should be taken into consideration. All the three phenyl zinc reagents give the same transmetallation product, Pd-Ph species, so it is reasonable to believe that the rate of breaking the Zn-C bond will affect the transmetallation rate. Higher reaction rate could be expected for phenylzinc reagent with weaker Zn-C bond and longer Zn-C bond distance especially in the case where the transmetallation undergoes a nucleophilic substitution pathway (Figure S5).

Alternatively, the transmetallation may go through a four-membered ring transition state in which the Pd and Zn are bridged by a halide anion (Figure S5). In this case, we also need to consider the Pd-X

interaction. As a soft acid, Pd^{2+} has a stronger affinity to I^- than Br^- and Cl^- , which suggests a lower activation energy for the formation of the four-membered ring transition state of $[\text{PhZnI}_2(\text{THF})]^-$.

It is also possible that transmetallation involves a five-membered ring transition state (Figure S5) in which the AcO^- bridges the Pd and Zn cations. It can be expected that the dissociation of the Zn-X bond gives an empty p orbital available for the formation of the five-membered ring transition state. In this case, the feasibility of breaking the Zn-X bond may also play a role in the transmetallation. I^- is the best leaving group among halide anions, so the lowest activation energy of $[\text{PhZnI}_2(\text{THF})]^-$ could be expected.

At the present time, we can't rule out any one out of the three discussed possibilities, but it should be noted that in all the three cases, breaking the Zn-C is playing an important role in the transmetallation. We are currently carrying out further detailed spectroscopic and theoretic investigations, and the results will be reported in the near future.

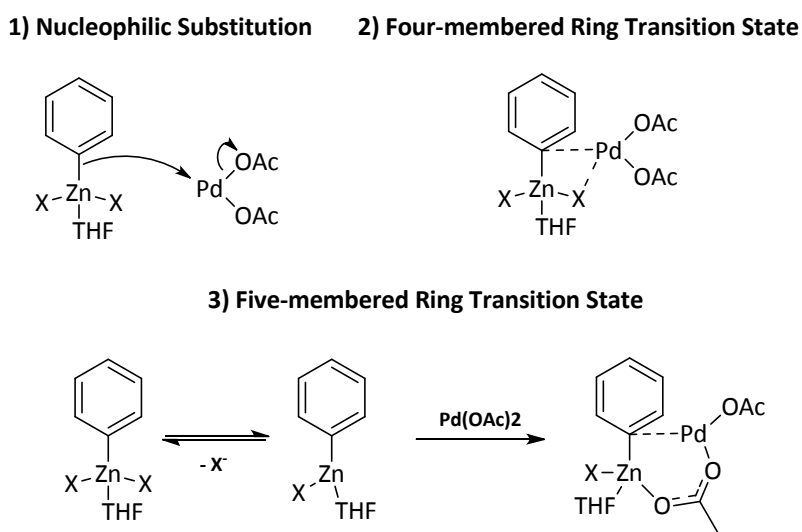


Figure S5 Possible transmetallation pathways.

References

1. R. C. Nelson and J. T. Miller, *Catal. Sci. Technol.*, 2012, **2**, 461-470.
2. C. Chieh and M. A. White, *Z. Kristallogr.*, 1984, **166**, 189-197.
3. J. Wong and F. W. Lytle, *J. Non-cryst. Solids*, 1980, **37**, 273-284.
4. G. Mosel, T. Hübert, M. Nofz, R. Brenneis, P. Köcher and G. Kley, *J. Mater. Sci.*, 2001, **36**, 5017-5025.
5. B. Ravel and M. Newville, *J. Synchrotron Radiat.*, 2005, **12**, 537-541.
6. T. Ressler, *J. Synchrotron Radiat.*, 1998, **5**, 118-122.
7. K. Fagnou and M. Lautens, *Angew. Chem. Int. Ed.*, 2002, **41**, 26-47.